Life Sciences 233 (2019) 116666

Contents lists available at ScienceDirect

Life Sciences

journal homepage: www.elsevier.com/locate/lifescie

Renoprotective effects of pirfenidone on chronic renal allograft dysfunction by reducing renal interstitial fibrosis in a rat model

Zhen-Zhen Qiu[a,1], Ji-Ming He[b,1], Hao-Xiang Zhang[c,1], Zuo-Hua Yu[b], Zhi-Wei Zhang[d], Hao Zhou[b,*]

[a] Department of Physical Education, Minjiang University, Fuzhou 350108, PR China
[b] Department of Urology, The Affiliated People's Hospital of Fujian University of Traditional Chinese Medicine (The People's Hospital of Fujian Province), Fuzhou 350004, PR China
[c] Department of Gastroenterology, General Hospital of Tibet Military Region PLA, Lhasa 850003, PR China
[d] Department of Research, Beijing Zhong Jian Dong Ke Company, Beijing 100176, PR China

ARTICLE INFO

Keywords:
Pirfenidone
Chronic renal allograft dysfunction
Renal fibrosis
Anti-inflammation
Anti-oxidation

ABSTRACT

Aim: Pirfenidone (PFD) has been used as medication for idiopathic pulmonary fibrosis due to its ability in reducing lung fibrosis. However, the underlying mode of action in renal fibrosis during chronic renal allograft dysfunction (CRAD) requires further investigation. Therefore, the present study was conducted to explore the effects of PFD on renal injury induced by CRAD.

Main methods: Initially, the CRAD rat model was established, followed by the intragastric administration of PFD to the rats. Urine and blood samples were collected and tested against indicators of renal functions. The renal tissues were microscopically observed to determine the changes in pathological morphology. The anti-inflammatory, anti-fibrotic and anti-oxidant properties of PFD were explored in the setting of CRAD.

Key findings: The success rate of model establishment was 92.31%, which was reflected by weight loss, appetite loss, faded fur, and retarded reaction, with the symptoms found to exacerbate with time. PFD treatment could improve renal function, ameliorate inflammation and renal fibrosis as well as promote the anti-oxidant ability of renal allograft, indicating its potential role as an effective therapeutic agent for CRAD.

Significance: In conclusion, PFD was found to have renoprotective effects on renal injury induced by CRAD, which resulted in the alleviation of inflammation and renal fibrosis, providing novelty for CRAD clinical treatment.

1. Introduction

In recent years, renal allograft transplant has been widely used as a promising treatment mode for chronic renal failure instead of dialysis since patients present with better prognosis and longer survival time [1]. However, the development of chronic renal allograft dysfunction (CRAD) is one of the major contributing factors affecting the survival of kidney transplant recipients [2]. CRAD can be attributed to injuries induced by immunological and non-immunological causes, characterized by pathological changes including tubular atrophy, fibrointimal hyperplasia, interstitial fibrosis, glomerulosclerosis and arteriolar hyalinosis [3]. Despite the application of effective immunosuppressants and sophisticated transplant techniques, long-term survival of renal allograft patients remains to be unsatisfactory [4]. Therefore, there is growing interest in developing novel therapeutic methods for the treatment of CRAD.

Pirfenidone (PFD) is an orally administered drug used for idiopathic pulmonary fibrosis to slow the progression of the disease in order to obtain well-functioning lungs, with a progression-free survival [5]. In addition to its immunosuppressive effects, PFD has also been characterized to have antifibrotic, antioxidant and anti-inflammatory properties [6]. In addition, there is evidence suggesting that PFD is a promising therapeutic agent for diabetic nephropathy with clinical features of inflammation and marked tubulointerstitial fibrosis [7]. More importantly, PFD could slow down the progression of renal fibrosis *i.e.* observable in renal diseases including chronic renal allograft injury, as reported in a previous study [8]. The renoprotective activity provided by this drug has also been documented in animal models and pathologies particularly against chronic renal failure, which was found to be through suppression of interstitial fibrosis [9]. Another study also

* Corresponding author at: Department of Urology, The Affiliated People's Hospital of Fujian University of Traditional Chinese Medicine, No. 602, Middle Road 817, Fuzhou 350004, Fujian Province, PR China
E-mail address: okhao@hotmail.com (H. Zhou).
[1] Zhen-Zhen Qiu, Ji-Ming He and Hao-Xiang Zhang have equal contribution.

https://doi.org/10.1016/j.lfs.2019.116666
Received 11 March 2019; Received in revised form 12 July 2019; Accepted 16 July 2019
Available online 17 July 2019
0024-3205/ © 2019 Elsevier Inc. All rights reserved.

demonstrated the ameliorative effects of PFD with inhibitory effects on mouse dendritic cell activation and function in both animal models and human patients after lung transplantation, highlighting its implication as potential therapy for restrictive allograft syndrome respectively [10,11]. Trials for clinical safety of PFD have also regarded its relative safe use for various demographics with chronic fibrotic disorders [12]. Given these literatures, the current study aims to investigate the cytoprotective effects of PFD in a uninephrectomized rat models in order to evaluate its use for CRAD treatment. This current study examined the effects of PFD on fibrosis, oxidation, and inflammation modulation, in order to provide a novel mechanism and scientific rationale for PFD mode of action to stabilize renal function during the treatment of CRAD.

2. Materials and methods

2.1. Ethics statement

All laboratory animals were used for medical research and all procedures were approved by the Ethics Committee of Fuzhou General Hospital.

2.2. Model establishment

A total of 65 male congenic Lewis rats were used as kidney graft recipients while 85 Specific Pathogen Free congenic Fischer (F344) rats served as donors. All rats (200–250 g, Beijing Vital River Laboratory Animal Technology Co., Ltd., Beijing, China) were housed in clean grade animal room. The CRAD models were established according to the method proposed by Poehnert et al. [13]. Since the Fischer-Lewis model has similar development after renal transplantation in humans, it has been intensively studied and widely accepted as an animal model of chronic renal allograft rejection, it was established in the present study [14].

2.3. Uninephrectomy surgery

Following the administration of general anesthesia with 3% sodium pentobarbital (30 mg/kg, Hangzhou Zhongmei Huadong Pharmaceutical Co., Ltd., Hangzhou, Zhejiang, China) on the F344 rats and Lewis rats, uninephrectomy surgery was conducted. A half-inch incision was made on the left flank portion of the abdomen, after which the perirenal fat was separated from the kidney with the use of blunt forceps. Next, the kidney was extracted from the abdomen, which separated the kidney from the surrounding fat and suprarenal gland. Next, the renal artery was ligated using a non-absorbable surgical suturing thread on the vein and ureter 0.5 cm below the level of hilum, followed by a snap resection of kidney. The uninephrectomized rats were injected with ceftriaxone for 3 days.

2.4. Kidney transplantation

Male Fischer (F344) (n = 65, weight: 200–250 g, age: 8–12 weeks) were used for this procedure. A surgical ASX-2 microscope was provided by Shanghai Anxin Optical Instrument Manufacture Co., Ltd., (Shanghai, China). The rats were intraperitoneally injected with 3% sodium pentobarbital (30 mg/kg). The left kidney was then removed from a recipient Lewis rat with the left renal vessels clamped. The left donor kidney was removed from a F344 rat, cooled and positioned in the recipient Lewis rat. The renal arteries, veins and ureters of the donor and recipient rats were anastomosed end-to-end with 10–0 prolene (Ningbo Lingqiao Biological Technology, Ningbo, Zhejiang, China), without the use of ureteral stents. Cyclosporine A (1.5 mg/kg/day; Novartis International AG, Basel, Switzerland) was administered at a low dose for 10 days after transplantation to inhibit acute rejection. The recipients were then given ceftriaxone (Rocephin; 20 mg/kg/day) intravenously for 3 days in case of infection. The right kidney of each recipient was resected 10 days post-surgery. Kidneys without significant transplant complications (including pyelonephritis or hydronephrosis) were selected for subsequent experiments [15]. Rats with obvious signs of surgery failure were excluded from the current study. There were 60 successfully established CRAD model rats. Following the transplantation, the rats were marked and subjected to rewarming treatment. Once the rats regained their normal activities, they were separately raised for 24 h.

2.5. Animal grouping

Drug administration was conducted 12 weeks after renal transplantation [5]. The rats were randomly assigned into 3 groups with 20 rats in each group: the prednisone group (rats were given prednisone from the beginning *via* intragastric administration, 100 mg/kg/day [16,17]), the PFD group (rats were given PFD suspension from the beginning *via* intragastric administration, 10 mg/kg/day) and the CRAD group (rats were given normal saline from the beginning *via* intragastric administration, 100 mg/kg/day). The PFD suspension was prepared by mixing normal saline and PFD at a ratio of 100:1. Administration was performed one once a day for 5 consecutive days. There were additional 20 Lewis male healthy rats that served as normal control (the normal group).

2.6. Sample selection

During the period following the successful CRAD model establishment and before administration of treatment, urine and blood preparation were harvested at 0 d, 10 d, 20 d, and 30 d post-administration. Urine specimen was collected using metal metabolic cages. Following collection, urine output was recorded. Then, 10 mL urine was subjected to centrifugation at 5000 r/min for 10 min with the dregs removed, sub-packed and preserved in a −80 °C refrigerator for further analysis. Blood preparation was obtained from orbital veniplex using a glass capillary (diameter: 1.0 mm). The whole blood was extracted and preserved in an Eppendorf tube at 4 °C overnight, followed by centrifugation at 4000 r/min for 10 min with the supernatant obtained and preserved in a −80 °C refrigerator for further analysis. Pathological renal samples were harvested and weighed at 0 d, 10 d, 20 d, and 30 d post-administration, after rats were euthanized.

2.7. Determination of routine biochemistry indicators

The 24-h urine protein excretion, blood urea nitrogen and serum creatinine were determined using urine protein kit (hj-C2309, Shanghai Lanpai biotechnology Co., Ltd., Shanghai, China), urea nitrogen kit (JKSJ-2205, Shanghai Jingkang Biotechnology Co., Ltd., Shanghai, China) and creatinine kit (B-TAE-233, Tianjin Anoric Bio-technology Co., Ltd., Tianjin, China), respectively.

2.8. Glomerular filtration rate (GFR) determination

The fluorescein isothiocyanate-inulin (100 mg/kg, Sigma-Aldrich Chemical Company, MO, USA) was administered into the rats intravenously *via* tail vein at 0 d, 10 d, 20 d and 30 d post-administration. Venous blood was extracted at 3 min, 7 min, 10 min, 15 min, 35 min, 55 min and 75 min post-injection. The fluorescent level was measured at the wavelengths of 480 nm and 530 nm using a Fluoroskan Ascent fluoroanalyzer (Thermo Fisher Scientific Inc., CA, USA). GFR was calculated with the use of a single-compartment model [18].

2.9. Pathomorphological observation of renal tissues

The harvested renal tissues were fixed in 10% neutral formaldehyde, conventionally embedded and sectioned into serial slices at

a thickness of 4 μm, followed by hematoxylin-eosin (HE) staining and Masson staining.

2.10. HE staining

Tissue sections were heated in an 80 °C oven for 1 h, cooled down, conventionally dehydrated using gradient alcohol, cleared by xylene and washed. Hematoxylin (H8070-5 g, Beijing Solarbio Life Sciences Co., Ltd., Beijing, China) was applied to slices for 4 min, followed by differentiation using hydrochloric ethanol for 10 s. The slices were washed for 5 min. Ammonia was used to re-stain slices for 10 min. Eosin (PT001, Shanghai Bogoo Biological Technology Co., Ltd., Shanghai, China) was subsequently used to stain slices for 2 min, followed by gradient alcohol dehydration and xylene clearing. The slices were then mounted by a neutral gum and the pathological changes and inflammatory cell infiltration were observed under an optical microscope (DMM-300D, Shanghai Caikon Optical Instrument Co., Ltd., Shanghai, China). A total of 5 visual fields in the upper left, upper right, lower left, lower right and middle part were observed in single blind trial under low magnification. The degree of renal interstitial fibrosis was evaluated by grading the vacuolar degeneration of renal tubular epithelial cells, tubular dilatation, tubular atrophy, red blood cell cast, protein cast, interstitial edema, interstitial fibrosis, and interstitial inflammatory cell infiltration. The mean value was obtained and regarded as the renal tubular interstitial injury index, with a higher index indicating a more serious fibrosis.

2.11. Masson staining

Following de-waxing and hydration, the sections were stained with Weigert hematoxylin for 5–10 min, differentiated with hydrochloric ethanol for several seconds and stained with Ponceau S acid solution for 5–10 min. Afterwards, 0.2% glacial acetic acid was used to briefly wash the sections and 1% molybdophosphoric acid was employed for differentiation for 3–5 min. The slices were then stained with aniline blue for 5 min, briefly washed again with 0.2% glacial acetic acid, dehydrated, permeabilized and mounted. Ten fields were randomly selected from the injured area of each section under a microscope (×400). The Image-pro Plus 6.0 (Media Cybernatics, USA) was used for image analysis to determine the collagen volume fraction using the following formula: collagen volume fraction = the collagen area / the injured area. After Masson staining, 5 non-overlapping renal tubular interstitial fields were randomly selected (×400) to calculate the relative area of renal tubular interstitial fibrosis. The mean value was obtained for semi-quantitative analysis. The renal tubular interstitial fibrosis was graded using 5 categories as follows: 0 = normal, 1 = the area of renal tubular interstitial fibrosis < 25%, 2 = 25% < the area of renal tubular interstitial fibrosis < 49%, 3 = 50% < the area of renal tubular interstitial fibrosis < 75% and 4 = the area of renal tubular interstitial fibrosis > 75%.

2.12. Western blot analysis

The concentrations of proteins extracted from tissues and cells were determined using the bicinchoninic acid Protein Assay Kit (Wuhan Boster Biological Technology Co., Ltd., Wuhan, Hubei, China) according to the manufacturer's instructions. The proteins that were extracted were mixed with the loading buffer, boiled at 95 °C for 10 min, after which 30 μg protein was loaded to each well. The 10% polyacrylamide gel (Wuhan Boster Biological Technology Co., Ltd., Wuhan, Hubei, China) electrophoresis was performed to separate the protein with the voltage changed from 80 V to 120 V. The protein was then transferred to a polyvinylidene fluoride membrane (100 mV for 45–70 min). The membrane was blocked with 5% bovine serum albumin (BSA) for 1 h, after which incubation was carried out with the following rabbit polyclonal antibodies overnight at 4 °C: transforming growth factor-β (TGF-β) (1:1000, ab92486), IL-2 (1:1000, ab25104), tumor necrosis factor-α (TNF-α) (1:2000, ab6671), matrix metalloprotein-9 (MMP-9) (1:1000, ab38898) and Vimentin (1:3000, ab137321). After receiving 3 washes (5 min each) with Tris-buffered saline with Tween 20 (TBST), the membrane was incubated with goat anti-rabbit Immunoglobulin G (IgG) secondary antibody (1:10000, ab205718) at room temperature for 1 h, followed by additional 3 washes with TBST (5 min each). All the aforementioned antibodies were purchased from Abcam Inc., (Shanghai, China). Proteins were detected by chemiluminescence, and images were acquired using the Gel Doc EZ imager (Bio-Rad, CA, USA). Target protein bands were quantified using ImageJ software with glyceraldehyde-3-phosphate dehydrogenase (GAPDH) used as the internal control.

2.13. Immunohistochemistry

The sections were dewaxed, hydrated and incubated with 3% H_2O_2 at room temperature for 10 min. Antigen retrieval was conducted using microwave method. The sample was blocked with 5% BSA for 1 h. Next, primary antibodies, including MMP-9 (1: 100, ab38898, Abcam Inc., Shanghai, China) and Vimentin (1: 100, ab137321, Abcam Inc., Shanghai, China) were added and incubation was carried out with the sample at 4 °C overnight, followed by a wash with phosphate buffer saline (PBS). Subsequently, biotin-labeled IgG was added as the secondary antibody and incubated with the sample for 30 min. Streptavidin peroxidase agent was added dropwise and incubated with the sample for 60 min. Following coloration by diaminobenzidine, the sample was slightly stained with hematoxylin, dehydrated, cleared and mounted. During the staining period, PBS or nonimmune serum was used to replace the primary antibody as the negative control. Ten fields were randomly selected from the injured area of each section under a microscope and the number of positive-stained cells was calculated in each field.

2.14. Reverse transcription quantitative polymerase chain reaction (RT-qPCR)

Total RNA was extracted using Trizol method. The cDNA was synthesized according to the instructions of High Capacity cDNA Reverse Transcription kit (Applied Biosystems, Foster City, USA). RT-qPCR was performed with the aids of Power SYBR® Green Master mix (Applied Biosystems, Foster City, USA) and StepOne™ Real-Time PCR System (Applied Biosystems, Foster City, USA). Three duplicated wells were set for each pair of primers. The primer sequences are shown in Table 1.

2.15. Measurement of superoxide dismutase (SOD), glutathione peroxidase (GSH-Px) and malondialdehyde (MDA)

SOD activity was measured by adapting the Sun et al. (1988) method [19]. The tissues were homogenized in cold isotonic saline solution and the homogenate was centrifuged at 10000 ×*g* for 10 min

Table 1
Primer sequences for reverse transcription quantitative polymerase chain reaction.

Primer name	Primer sequence (5′-3′)
Vimentin	F: 5′-ACATCCACCGCACCTAC-3′ R: 5′-CAACTCCCTCATCTCCTCCTC-3′
MMP-9	F: 5′-CAGACCAAGGGTACAGCCTGT-3′ R: 5′-AGCGCATGGCCGAACTC-3′
GAPDH	F: 5′-AACGACCCCTTCATGAC-3′ R: 5′-TCCACGACATACTCAGCA-3′

Note: MMP, matrix metalloprotein; GAPDH, glyceraldehyde-3-phosphate dehydrogenase; F, forward; R, reverse.

at 4 °C. The measurement of SOD was based on the inhibitory effects of SOD on generating agent of superoxide anion to reduce nitroblue tetrazolium. The maximum absorbance value was detected at 560 nm.

GSH-Px activity was determined according to Flohé and Gunzler (1984) method [20]. The tissues were homogenized in cold buffer solution, which was prepared by mixing 0.1 m KH_2PO_4/K_2HPO_4 (pH = 7.0) and 29.2 mg ethylenediaminetetraacetic acid in 100 mL distilled water and 10.0 mg digicitrin in 100 mL distilled water with the final volume of 2000 mL. Subsequently, centrifugation was carried out at 10000 ×*g* for 10 min at 4 °C. GSH-Px was determined based on nicotinamide adenine dinucleotide phosphate oxidation to NAD^+, which was catalyzed by GSH reductase of limiting concentration, and then absorbance was read at a maximum level at 340 nm.

The tissues were homogenized in 20 mM Tris-HCl buffer solution (pH = 7.4), followed by centrifugation at 10000 ×*g* for 10 min at 4 °C. The supernatant was obtained and the content of lipid peroxidation (LPO) was measured using Bioxytech LPO-586 kit (OXIS International, Portland, USA). The chromatogenic agent was employed for the kit and reacted with MDA and 4-hydroxyalkenals at (45 ± 1)°C to produce stable chromophore with maximum absorbance value, which was detected at 586 nm.

2.16. Statistical analysis

Statistical analyses were performed using SPSS 21.0 (IBM Corp., Armonk, NY, USA). Measurement data with normal distribution were presented as the mean ± standard deviation, while those with skewed distribution or heterogeneity of variance were expressed as interquartile range. Data at different time points were compared by two-way analysis of variance (ANOVA). Comparison at the same time point among multiple groups was conducted with the use of one-way ANOVA. A value of $p < 0.05$ was considered statistically significant.

3. Results

3.1. The rat models of CRAD were successfully established

Initially, a rat model for CRAD was established. Compared with the rats in the normal group, there was no significant difference observed regarding the GFR of rats in the CRAD group at 0 d treatment post-administration (Fig. 1D), indicating the successful establishment of the rat models. The success rate was 92.31% out of the 65 rats that were initially enrolled in the study. Subsequently, the rats were randomly grouped into the CRAD, prednisone and PFD groups with 20 rats in each group. Rats in the normal group were provided with a normal diet with normal water intake and had no change in weight. Post-surgery, rats in the CRAD group were found with stunted response, bad appetite, decreased drinking, reduced weight by 35% and less self-conscious activities while their fur became yellow, scarcer and lusterless. These symptoms became more evident over time. Rats in the PFD group presented with much better behavior and self-cleaning with only 20% weight loss in comparison to rats in the CRAD group. No significant difference was observed between the prednisone and PFD groups (Fig. 2). These findings indicated the successful establishment of rat model with CRAD.

3.2. PFD has therapeutic effects on rats with CRAD

The effects of PFD on renal function of rats with CRAD were investigated by measuring serum creatinine, blood urea nitrogen, 24-h urine protein excretion and GFR at 0 d, 10 d, 20 d and 30 d post-administration of treatments. The results revealed an increase in serum creatinine, serum urea nitrogen, and 24-h urine protein excretion (Fig. 1A–C, $p < 0.05$) while GFR decreased in the CRAD group compared to the normal group (Fig. 1D, $p < 0.05$). In addition, the renal functions of rats in the CRAD group started to weaken through time, as indicated by the increased urine protein. However, compared with the CRAD group, the rats in the prednisone and PFD groups presented with

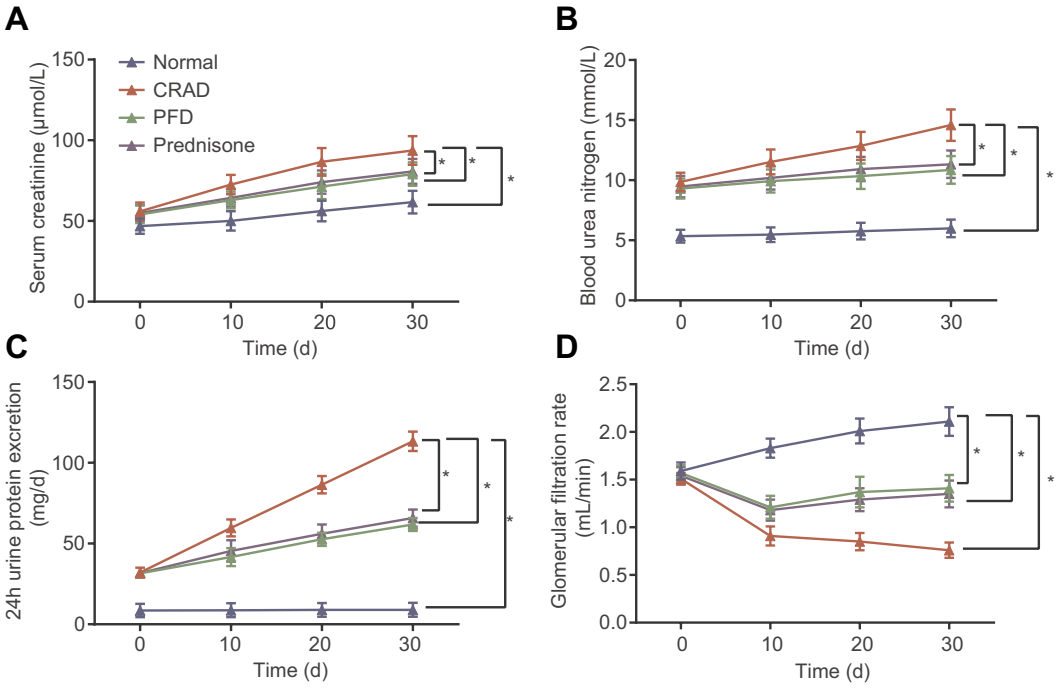

Fig. 1. PFD has therapeutic effects on rats with CRAD. A, the serum creatinine levels at different time points, n = 5, *$p < 0.05$. B, the blood urea nitrogen levels at different time points, n = 5, *$p < 0.05$. C, 24-h urine protein excretions at different time points, n = 5, *$p < 0.05$. D, glomerular filtration rates at different time points, n = 5, *$p < 0.05$. The data were measurement data and expressed as mean ± standard deviation. Comparison at different time points was conducted by two-way ANOVA.

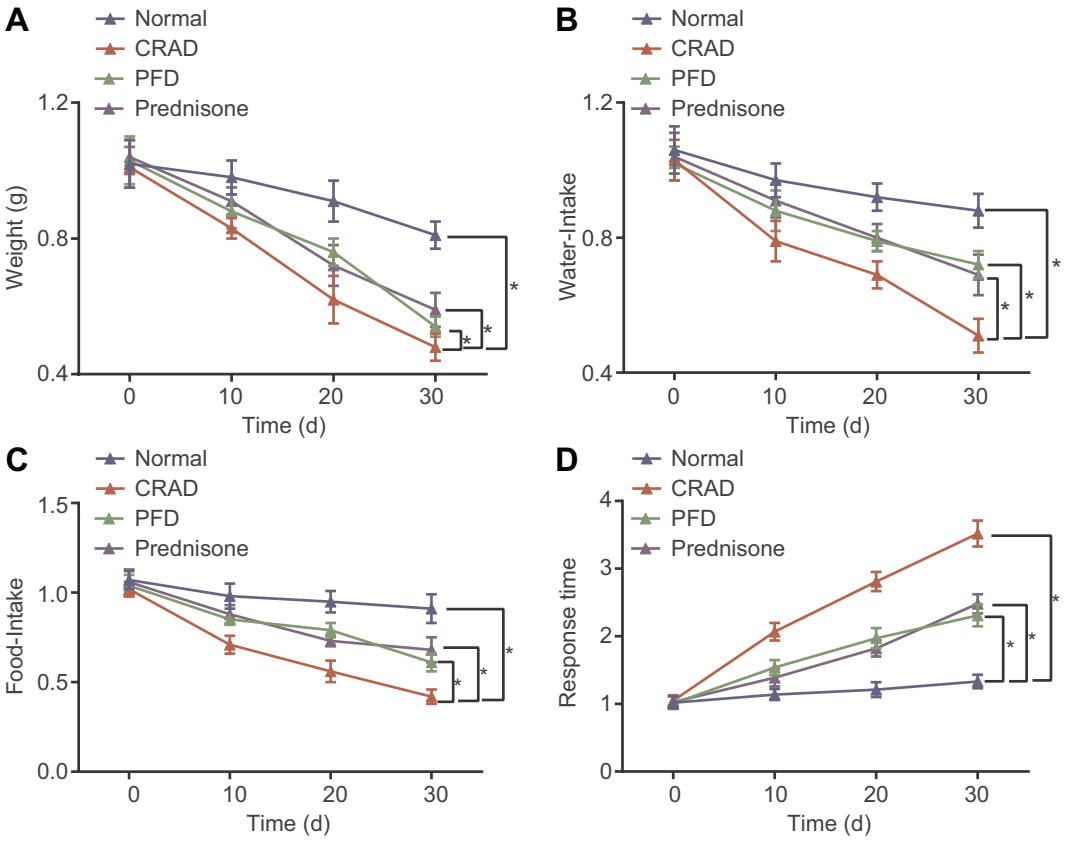

Fig. 2. The rat models of CRAD were successfully established. A, body weight of rats at 10 d, 20 d and 30 d, n = 5. B, water-intake of rats at 10 d, 20 d and 30 d, n = 5. C, food-intake of rats at 10 d, 20 d and 30 d, n = 5. D, correct reaction time of rats at 10 d, 20 d and 30 d, n = 5. *$p < 0.05$. Comparison at different time points was conducted by two-way ANOVA while comparison among multiple groups at the same time point was analyzed by one-way ANOVA.

lower serum creatinine, blood urea nitrogen, and 24-h urine protein excretion along with higher GFR ($p < 0.05$). Meanwhile, there was no significant difference found between the prednisone and PFD groups ($p > 0.05$). These findings indicated that PFD can improve the renal function of rats with CRAD.

3.3. PFD alleviates renal injury and inflammatory response in rats with CRAD

In order to explore the effects of PFD on the pathological changes of renal tissues of rats, HE staining (Fig. 3A–B) and Masson staining (Fig. 3C–D) were performed. The results revealed that there were no evident pathological changes present in the normal group with renal tubular epithelial cells well-developed and renal tubule was small without inflammatory cell infiltration in the interstitial tissues. However, the renal tissues were significantly enlarged in the CRAD group, with vacuolar degeneration and dilatation present in some of the renal tubular epithelial cells along with renal tubular epithelial cell atrophy, necrosis, and detachment with widened interstitium. Moreover, mononuclear cells and lymphocytes infiltration where found microscopically. Fibroblast hyperplasia and renal interstitial fibrosis were also observed in the interstitial tissues of CRAD. The aforementioned findings aggravated with time. According to the Masson staining, the CRAD group exhibited much more blue-stained collagen fibrils in interstitium as time progressed with fading red stained tubular epithelial cells, indicating aggravated tubulointerstitial fibrosis and injured renal tubular epithelial cells. Compared with the normal group, both the renal tubular interstitial injury index and renal interstitial fibrosis area index were significantly higher in the CRAD group ($p < 0.05$). However, groups that had received treatment with prednisone and PFD exhibited ameliorated renal injury and renal interstitial fibrosis in comparison to the CRAD group as indicated by significantly lower renal tubular interstitial injury index and renal interstitial fibrosis area index ($p < 0.05$); no significant difference was observed between the prednisone and PFD groups. The results demonstrated that PFD could alleviate renal injury and renal interstitial fibrosis.

Subsequently, Western blot analysis was conducted to determine the expression levels of TGF-β, interleukin-2 (IL-2) and TNF-α in renal tissues of rats at different time points. Compared with the normal group, expression levels of TGF-β, IL-2 and TNF-α all increased in the CRAD group (Fig. 1E–G, $p < 0.05$) and continued to rise as time progressed. In contrast, opposite changes were found in the prednisone and PFD treated groups ($p < 0.05$) while expression levels of TGF-β, IL-2 and TNF-α did not differ significantly between the two groups ($p > 0.05$). These further highlighted the improvement in the inflammatory response of CRAD model rats following treatment with PFD.

3.4. PFD improves renal interstitial fibrosis of rats with CRAD

In order to investigate the effects of PFD on renal interstitial fibrosis, immunohistochemistry was employed to the quantify MMP-9 and Vimentin in renal tissues. The results showed that there were higher levels in MMP-9 and Vimentin in the CRAD group compared to the normal group (Fig. 4A–B, $p < 0.05$) and this continued to increase with time. However, CRAD rat models treated with prednisone and PFD both showed significantly lowered levels of MMP-9 and Vimentin ($p < 0.05$) than the CRAD models while these effects of prednisone and PFD were not significantly different. Next, RT-qPCR and Western blot analysis were performed to determine the mRNA and protein expression of MMP-9 and Vimentin for further verification. The results revealed were the same whereby expression of MMP-9 and Vimentin

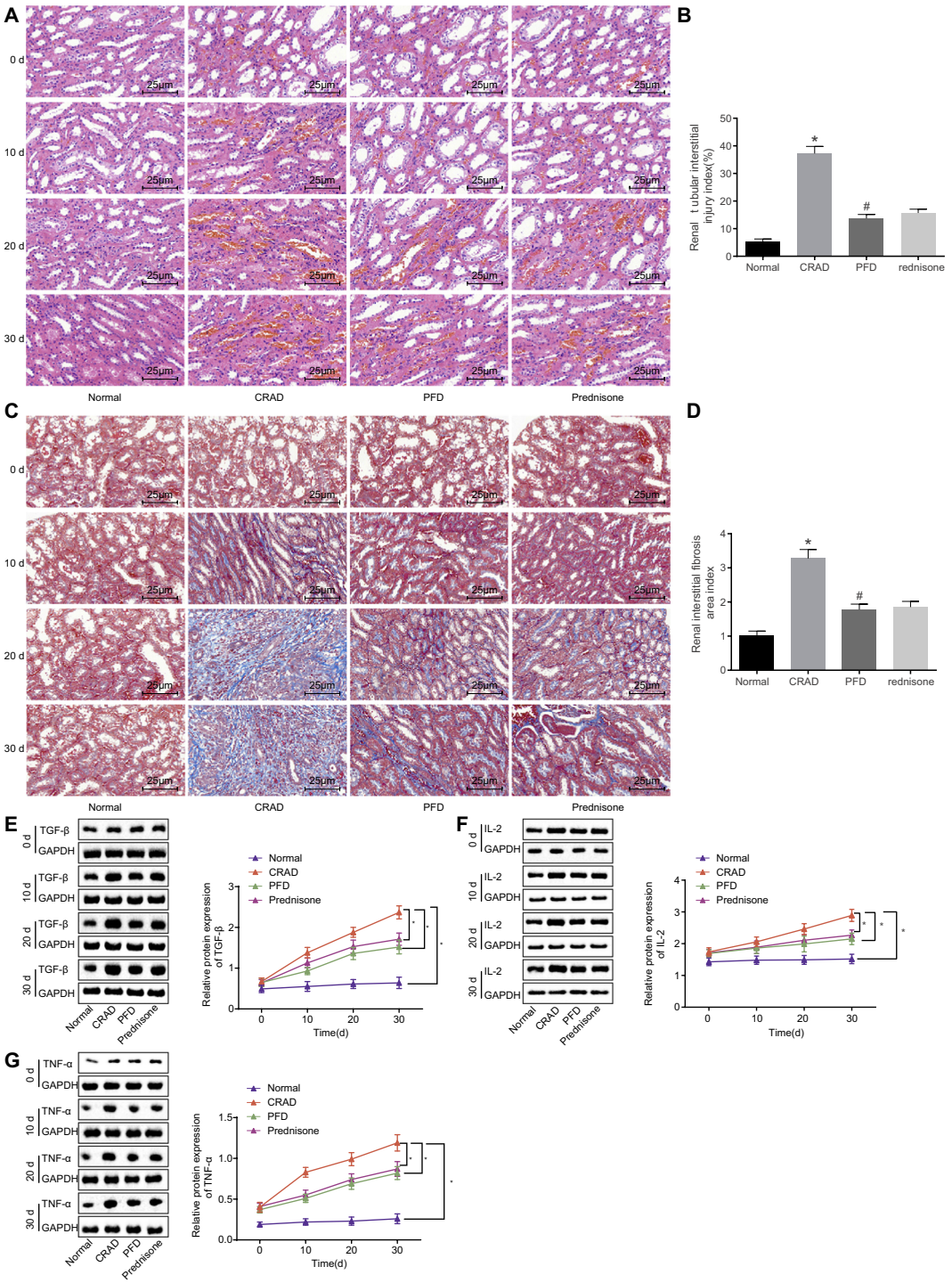

Fig. 3. PFD alleviates renal injury and inflammatory response in rats with CRAD. A, pathological changes of renal tissues identified by HE staining, n = 5, ×400, scale bar = 25 μm. B, renal tubular interstitial injury index of rats at 30 d, n = 5, *$p < 0.05$ *vs.* the normal group (rats without any treatment), #$p < 0.05$ *vs.* the CRAD group (rats with CRAD), one-way ANOVA was introduced for data analysis. C, fibrosis of renal tissues identified by Masson staining, n = 5, ×400, scale bar = 25 μm. D, renal interstitial fibrosis area index of rats at 30 d, n = 5, *$p < 0.05$ *vs.* the normal group (rats without any treatment), #$p < 0.05$ *vs.* the CRAD group (rats with CRAD), one-way ANOVA was introduced for data analysis. EFG, the protein levels of TGF-β, IL-2 and TNF-α determined by Western blot analysis, n = 5, *$p < 0.05$. The data were measurement data and expressed as mean ± standard deviation. Comparison at different time points was conducted by two-way ANOVA.

increased in the CRAD group than that in the normal group (Fig. 4C–F, $p < 0.05$) and these changes were exacerbated with time. Meanwhile, the opposite results were observed in the prednisone and PFD treated groups ($p < 0.05$) with no significant difference detected between the two groups. Evidently, the aforementioned results demonstrated that PFD could improve renal interstitial fibrosis of rats with CRAD.

3.5. PFD enhances the antioxidant ability of renal allograft in rats with CRAD

Lastly, the regulatory functions of PFD on the antioxidant ability of renal allograft in rats with CRAD were determined through the measurement of the levels of SOD, GSH-Px and MDA. It was found that

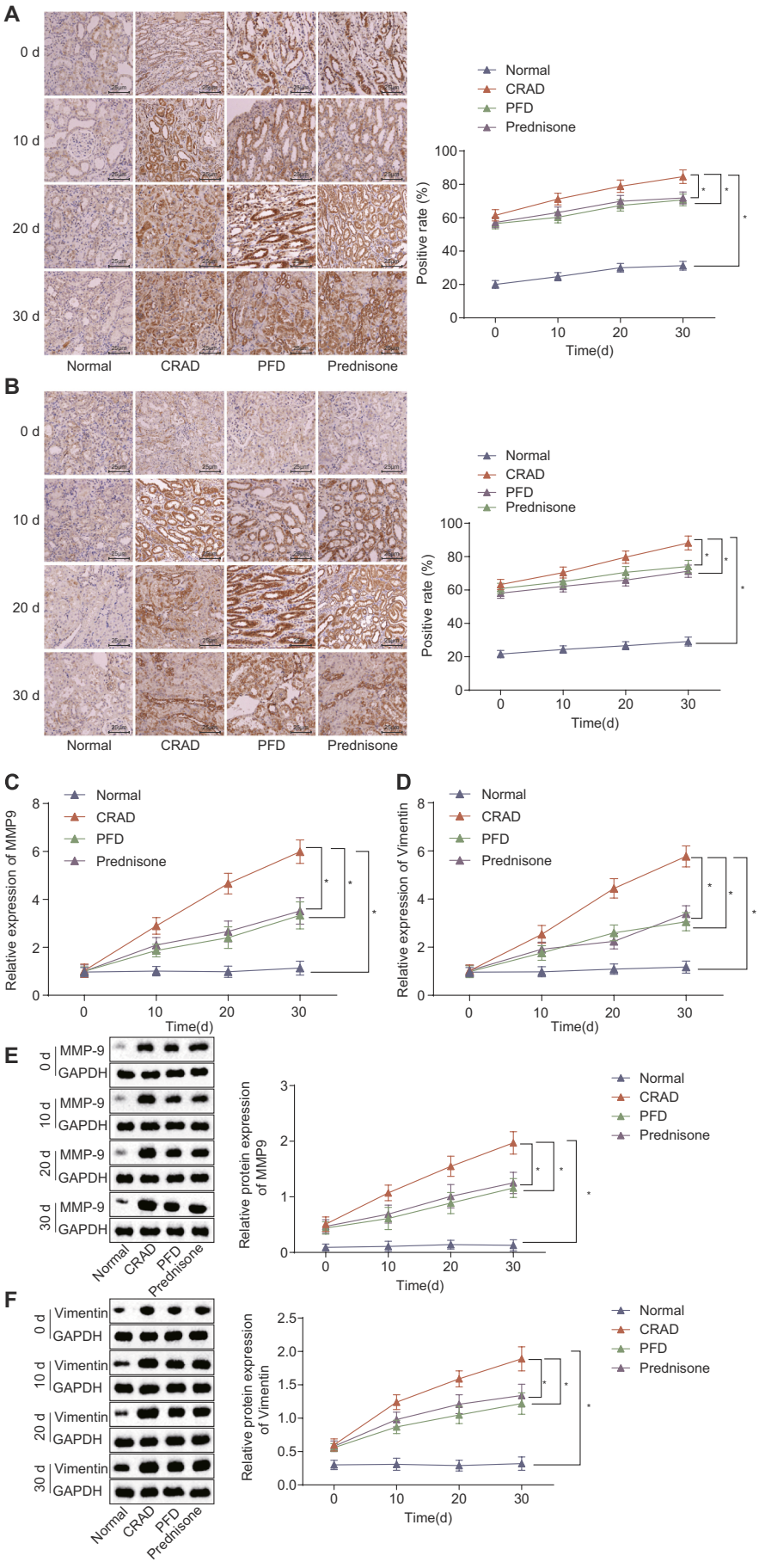

(caption on next page)

Fig. 4. PFD improves renal interstitial fibrosis of rats with CRAD. AB, protein levels of MMP-9 and Vimentin in renal tissues detected by immunohistochemistry, n = 5, ×400, scale bar = 25 μm. CD, mRNA expression of MMP-9 and Vimentin in renal tissues determined by RT-qPCR, n = 5, $*p < 0.05$; EF, protein levels of MMP-9 and Vimentin in renal tissues determined by Western blot analysis, n = 5, $*p < 0.05$. The data were measurement data and expressed as mean ± standard deviation. Comparison at different time points was conducted by two-way ANOVA.

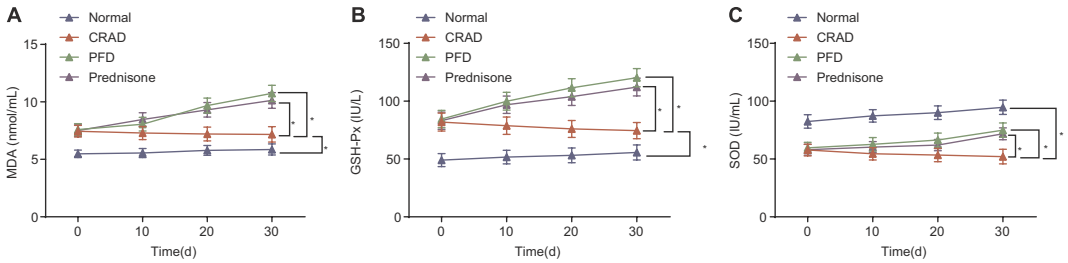

Fig. 5. PFD enhances the antioxidant ability of renal allograft in rats with CRAD. A, SOD activity at different time points. B, GSH-Px activity at different time points. C, MDA levels at different time points. n = 5. $*p < 0.05$. The data were measurement data and expressed as mean ± standard deviation. Comparison at different time points was conducted by two-way ANOVA.

there was an increase in the levels of SOD and GSH-Px in the CRAD group compared with the normal group (Fig. 5A–B, $p < 0.05$) while MDA level decreased (Fig. 5C, $p < 0.05$). However, the levels of SOD, GSH-Px and MDA all reduced with the progression of time, while these factors were significantly higher in the prednisone and PFD treated groups compared with the CRAD group ($p < 0.05$) but it did not differ significantly between the two. These findings provided evidence that PFD resulted in the enhancement of antioxidant ability of renal allograft in rats with CRAD.

4. Discussion

CRAD is the predominant reason for the renal graft failure in the first decade following transplantation [1]. Fortunately, PFD has been found to have anti-inflammatory and anti-oxidative properties that could potentially alleviate such renal injury [21]. Furthermore, patients with idiopathic pulmonary fibrosis who received treatment with PFD were documented to have longer period of progression-free survival [22]. Thus, we conducted the present study with the main purpose of investigating the anti-fibrotic, anti-inflammatory, and anti-oxidant effects of PFD administered following uninephrectomy surgery in order to determine the underlying mechanisms of its renoprotective action. The findings from our study provided additional evidence supporting the renoprotective effects of PFD against CRAD in rat models.

Renal interstitial fibrosis was significantly improved with PFD treatment as indicated by lower levels of MMP-9 and Vimentin. Renal fibrosis typically presents with the presence of extracellular matrix (ECM) components breaching the interstitium and glomerulus, the mechanism of which is mediated by ECM degradation and production [23]. Metalloproteinases or MMPs and their tissue inhibitors have been identified as crucial regulators of ECM homeostasis [24]. This anti-fibrotic property of PFD through the regulation of MMP imbalance has been consistently reported [21]. MMP family consists of a group of zinc-containing enzymes, including matrilysin and gelatinases; therefore, MMP-9 is associated with the regulation of renal fibrosis in cases of diabetic nephropathy [24]. Similarly, there is a reduction in the mRNA expression level and activity of MMP-9 following the addition of PFD in cardiac fibroblasts, resulting in the inhibition of adverse myocardial remodeling [25]. Vimentin (57 kDa) is a protein localized in cells with mesenchymal origin that plays a functional role as an intermediate filament and as also been found to be expressed in glomeruli, tubules and endothelial cells of renal allografts [26]. A previous study identified urinary mRNA level of Vimentin as an independent noninvasive biomarker to track the progression of renal fibrosis and the presence of higher Vimentin expression indicates severe fibrosis in renal tissues [27]. Therefore, our results regarding the anti-fibrotic property of PFD, as validated by previous works provide an insight regarding the underlying mechanism of the renoprotective effects of PFD.

In addition, the anti-inflammatory property of PFD in rats with CRAD was also investigated. The findings showed lower levels of TGF-β, IL-2 and TNF-α indicating the improvement of inflammatory reaction following PFD administration. Inflammation plays a crucial role in the progression of renal interstitial fibrosis and the pro-inflammatory cytokine, TNF-α, should be significantly suppressed in order to attenuate renal interstitial inflammation and fibrosis [28]. The inflammation-antagonizing effects of PFD have been previously demonstrated to occur through the inhibition of the expression of inflammatory regulators such as TNF-α and IL-1β both *in vivo* and *in vitro* [21]. Furthermore, TGF-β1 has been observed to be up-regulated in renal injury [29] while the antagonistic functions of PFD to TGF-β have been established in previous work [9]. Lastly, the increase of IL-2 in renal tissues in combination with TGF-β1 has also been implicated with the occurrence of renal structural damage and fibrosis [30]. These literatures support our findings regarding the anti-inflammatory property of PFD in CRAD.

The renoprotective potential of PFD extended to its antioxidant activity by which SOD, GSH-Px and MDA contents significantly increased following treatment. Oxidative stress is highly associated with an increased risk for acute rejection, impaired graft function, primary graft dysfunction or initial graft malfunction, thus lowering oxidative injuries is important to maintain long term post-transplant renal function [31]. Moreover, patients suffering from chronic renal disease have been found with suppressed activity of SOD [32]. Fortunately, PFD has been found to reduce oxidative stress by promoting the MDA activity and increasing GSH content in renal proximal tubular cells of 5/6 nephrectomized rats [33]. The potential of PFD in the mediation of intracellular antioxidants has been noted in idiopathic pulmonary fibrosis to alleviate fibrosis degree involving the equilibrium between nuclear factor erythroid-related factor 2 and broad-complex, tramtrack and bric-a-brac (BTB) and cap'n'collar protein (CNC) homology 1 (Bach1) [34]. However, due to the limited time and funding, more mechanistic work could not be conducted in the present study and therefore requires further investigation, which will be the emphasis of our future research. These results suggest that PFD exerts anti-oxidative properties conducive to the improvement of CRAD.

5. Conclusions

Taken together, the findings from our study provide a better understanding on the renoprotective property of PFD using rat models of CRAD. The current work demonstrated that PFD has anti-fibrotic, anti-inflammatory, and anti-oxidant properties on renal tissues against

CRAD following uninephrectomy surgery. Therefore, PFD might be a potentially new therapeutic option for CRAD. Nevertheless, the research is currently still in the preclinical stage, and the investigation on the detailed mode of action of PFD requires further investigation.

Declaration of Competing Interest

The authors declare that there are no conflicts of interest.

Acknowledgements

This study was supported by Natural Science Foundation of Fujian Province (2017J01313) and National Natural Science Foundation of China (81473496).

References

[1] W.M. Hamza, H.H. Ali, S.M. Gabal, S.A. Fadda, Chronic renal allograft dysfunction in Egyptian population: histopathological and immunohistochemical study, Saudi J. Kidney Dis. Transpl. 27 (2016) 921–928.
[2] Q. Yan, H. Jiang, B. Wang, W. Sui, H. Zhou, G. Zou, Expression and significance of RANTES and MCP-1 in renal tissue with chronic renal allograft dysfunction, Transplant. Proc. 48 (2016) 2034–2039.
[3] S. Assadiasl, P. Ahmadpoor, M. Nafar, M. Lessan Pezeshki, F. Pourrezagholi, M. Parvin, A. Shahlaee, A. Sepanjnia, M.H. Nicknam, A. Amirzargar, Regulatory T cell subtypes and TGF-beta1 gene expression in chronic allograft dysfunction, Iran. J. Immunol. 11 (2014) 139–152.
[4] Q. Yan, B. Wang, W. Sui, G. Zou, H. Chen, S. Xie, H. Zou, Expression of GSK-3beta in renal allograft tissue and its significance in pathogenesis of chronic allograft dysfunction, Diagn. Pathol. 7 (2012) 5.
[5] T.E. King Jr., W.Z. Bradford, S. Castro-Bernardini, E.A. Fagan, I. Glaspole, M.K. Glassberg, E. Gorina, P.M. Hopkins, D. Kardatzke, L. Lancaster, D.J. Lederer, S.D. Nathan, C.A. Pereira, S.A. Sahn, R. Sussman, J.J. Swigris, P.W. Noble, A.S. Group, A phase 3 trial of pirfenidone in patients with idiopathic pulmonary fibrosis, N. Engl. J. Med. 370 (2014) 2083–2092.
[6] E.S. Kim, G.M. Keating, Pirfenidone: a review of its use in idiopathic pulmonary fibrosis, Drugs 75 (2015) 219–230.
[7] K. Sharma, J.H. Ix, A.V. Mathew, M. Cho, A. Pflueger, S.R. Dunn, B. Francos, S. Sharma, B. Falkner, T.A. McGowan, M. Donohue, S. Ramachandrarao, R. Xu, F.C. Fervenza, J.B. Kopp, Pirfenidone for diabetic nephropathy, J. Am. Soc. Nephrol. 22 (2011) 1144–1151.
[8] J.F. Chen, H.F. Ni, M.M. Pan, H. Liu, M. Xu, M.H. Zhang, B.C. Liu, Pirfenidone inhibits macrophage infiltration in 5/6 nephrectomized rats, Am. J. Physiol. Renal Physiol. 304 (2013) F676–F685.
[9] K. Takakuta, A. Fujimori, T. Chikanishi, A. Tanokura, Y. Iwatsuki, M. Yamamoto, H. Nakajima, M. Okada, H. Itoh, Renoprotective properties of pirfenidone in subtotally nephrectomized rats, Eur. J. Pharmacol. 629 (2010) 118–124.
[10] P. Bizargity, K. Liu, L. Wang, W.W. Hancock, G.A. Visner, Inhibitory effects of pirfenidone on dendritic cells and lung allograft rejection, Transplantation 94 (2012) 114–122.
[11] R. Vos, S.E. Verleden, D. Ruttens, E. Vandermeulen, J. Yserbyt, L.J. Dupont, D.E. Van Raemdonck, N. De Raedt, O. Gheysens, P.A. De Jong, G.M. Verleden, B.M. Vanaudenaerde, Pirfenidone: a potential new therapy for restrictive allograft syndrome? Am. J. Transplant. 13 (2013) 3035–3040.
[12] M.E. Cho, J.B. Kopp, Pirfenidone: an anti-fibrotic therapy for progressive kidney disease, Expert Opin. Investig. Drugs 19 (2010) 275–283.
[13] D. Poehnert, V. Broecker, M. Mengel, B. Nashan, M. Koch, Induction of chronic renal allograft dysfunction in a rat model with complete and exclusive MHC incompatibility, Transpl. Immunol. 22 (2010) 137–143.
[14] E. Song, H. Zou, Y. Yao, A. Proudfoot, B. Antus, S. Liu, L. Jens, U. Heemann, Early application of Met-RANTES ameliorates chronic allograft nephropathy, Kidney Int. 61 (2002) 676–685.
[15] Q. Zhou, D. Lv, Y. Xia, Z. Zhao, H. Zhou, Decreased expression of sirtuin 3 protein correlates with early stage chronic renal allograft dysfunction in a rat kidney model, Exp. Ther. Med. 15 (2018) 3725–3732.
[16] W. Xu, Z. Lin, C. Yang, Y. Zhang, G. Wang, X. Xu, Q. Lv, Y. Ren, Y. Dong, Immunosuppressive effects of demethylzeylasteral in a rat kidney transplantation model, Int. Immunopharmacol. 9 (2009) 996–1001.
[17] F. Verhoeven, C. Prati, P. Totoson, R. Bordy, D. Wendling, C. Demougeot, Structural efficacy of NSAIDs, COX-2 inhibitor and glucocorticoid compared with TNFα blocker: a study in adjuvant-induced arthritis rats, Rheumatology 58 (2019) 1099–1103.
[18] B. Frennby, G. Sterner, Contrast media as markers of GFR, Eur. Radiol. 12 (2002) 475–484.
[19] Y. Sun, L.W. Oberley, Y. Li, A simple method for clinical assay of superoxide dismutase, Clin. Chem. 34 (1988) 497–500.
[20] L. Flohe, W.A. Gunzler, Assays of glutathione peroxidase, Methods Enzymol. 105 (1984) 114–121.
[21] X. Ji, Y. Naito, H. Weng, X. Ma, K. Endo, N. Kito, N. Yanagawa, Y. Yu, J. Li, N. Iwai, Renoprotective mechanisms of pirfenidone in hypertension-induced renal injury: through anti-fibrotic and anti-oxidative stress pathways, Biomed. Res. 34 (2013) 309–319.
[22] H. Huang, H.P. Dai, J. Kang, B.Y. Chen, T.Y. Sun, Z.J. Xu, Double-blind randomized trial of pirfenidone in Chinese idiopathic pulmonary fibrosis patients, Medicine (Baltimore) 94 (2015) e1600.
[23] W. Fu, Y. Wang, Z. Jin, H. Wang, W. Cheng, H. Zhou, P. Yin, W. Peng, Losartan alleviates renal fibrosis by down-regulating HIF-1alpha and up-regulating MMP-9/TIMP-1 in rats with 5/6 nephrectomy, Ren. Fail. 34 (2012) 1297–1304.
[24] J. Wang, Y. Gao, M. Ma, M. Li, D. Zou, J. Yang, Z. Zhu, X. Zhao, Effect of miR-21 on renal fibrosis by regulating MMP-9 and TIMP1 in kk-ay diabetic nephropathy mice, Cell Biochem. Biophys. 67 (2013) 537–546.
[25] Q. Shi, X. Liu, Y. Bai, C. Cui, J. Li, Y. Li, S. Hu, Y. Wei, In vitro effects of pirfenidone on cardiac fibroblasts: proliferation, myofibroblast differentiation, migration and cytokine secretion, PLoS One 6 (2011) e28134.
[26] D. Besarani, L. Cerundolo, J.D. Smith, J. Procter, M.C. Barnardo, I.S. Roberts, P.J. Friend, M.L. Rose, S.V. Fuggle, Role of anti-vimentin antibodies in renal transplantation, Transplantation 98 (2014) 72–78.
[27] Y.H. Cao, L.L. Lv, X. Zhang, H. Hu, L.H. Ding, D. Yin, Y.Z. Zhang, H.F. Ni, P.S. Chen, B.C. Liu, Urinary vimentin mRNA as a potential novel biomarker of renal fibrosis, Am. J. Physiol. Renal Physiol. 309 (2015) F514–F522.
[28] Y. Tang, F. Zhang, L. Huang, Q. Yuan, J. Qin, B. Li, N. Wang, Y. Xie, L. Wang, W. Wang, K. Kwan, Z. Peng, G. Hu, J. Li, L. Tao, The protective mechanism of fluorofenidone in renal interstitial inflammation and fibrosis, Am J Med Sci 350 (2015) 195–203.
[29] N. Hu, J. Duan, H. Li, Y. Wang, F. Wang, J. Chu, J. Sun, M. Liu, C. Wang, C. Lu, A. Wen, Hydroxysafflor yellow a ameliorates renal fibrosis by suppressing TGF-beta1-induced epithelial-to-mesenchymal transition, PLoS One 11 (2016) e0153409.
[30] H.M. El-Gowelli, M.W. Helmy, R.M. Ali, M.M. El-Mas, Celecoxib offsets the negative renal influences of cyclosporine via modulation of the TGF-beta1/IL-2/COX-2/endothelin ET(B) receptor cascade, Toxicol. Appl. Pharmacol. 275 (2014) 88–95.
[31] S. Kumar, U. Sharma, A. Sharma, D.B. Kenwar, S. Singh, R. Prasad, M. Minz, Evaluation of oxidant and antioxidant status in living donor renal allograft transplant recipients, Mol. Cell. Biochem. 413 (2016) 1–8.
[32] R.C. Noleto Magalhaes, C. Guedes Borges de Araujo, V. Batista de Sousa Lima, J. Machado Moita Neto, N. do Nascimento Nogueira, D. do Nascimento Marreiro, Nutritional status of zinc and activity superoxide dismutase in chronic renal patients undergoing hemodialysis, Nutr. Hosp. 26 (2011) 1456–1461.
[33] J.F. Chen, H. Liu, H.F. Ni, L.L. Lv, M.H. Zhang, A.H. Zhang, R.N. Tang, P.S. Chen, B.C. Liu, Improved mitochondrial function underlies the protective effect of pirfenidone against tubulointerstitial fibrosis in 5/6 nephrectomized rats, PLoS One 8 (2013) e83593.
[34] Y. Liu, F. Lu, L. Kang, Z. Wang, Y. Wang, Pirfenidone attenuates bleomycin-induced pulmonary fibrosis in mice by regulating Nrf2/Bach1 equilibrium, BMC Pulm. Med. 17 (2017) 63.